Electronic Supplementary Material (ESI) for RSC Advances

Gold Nanoparticles Supported on the Periodic Mesoporous Organosilica of SBA-15 as Efficient and Reusable Catalyst for Selective Oxidation of Silanes to Silanols

Lina Ma, Wenguang Leng, Yaopeng Zhao, Yanan Gao,* and Hongdong Duan*

Dalian Institute of Chemical Physics, Chinese Academy of Sciences, 457 Zhongshan Road, Dalian 116023, China.

Supporting Information

Table of Contents

1. General information

All chemicals used were of analytical grade and used as received. 4-(Chloromethyl)phenyltrimethoxysilane (CTS), 2,2'-bipyridyl (BiPy), copper (I) chloride, triethylsianol (97%), triisopropylsilane (99%) and triisopropylsilanol (98%) were purchased from Sigma-Aldrich (USA). Triphenylsianol (98%), triphenylsiane (97%), t-butyldimethylsilane (95%), t-butyldimethylsilanol (99%) and dimethylphenylsiane (98%) were purchased from J&K. Tri-n-propylsilane (98%), triphenylsilane (99%), dimethylphenylsilane (97%) and dimethylphenylsilanol (97%) were purchased from Alfa Aesar. Tributylsilane (98%), triethylsilane (98%) and diphenylsilanediol (98%) were purchased from TCI. SBA-15 was obtained from the Laboratory of Advanced Materials at Fudan University, Shanghai, China.

All The Au loading of the catalysts were determined by inductively coupled plasma spectrometer (ICP) on an ICPS-8100 Instrument (Shimadzu Corporation), by analyzing of a known concentration of dry catalyst sample which was digested under microwave in a diluted HF-HCl solution.

Power X-ray diffraction (XRD) patterns were recorded on a Rigaku RINT D/Max 2500 powder diffraction system, using a CuKα radiation (λ=0.15432nm) as X-ray source. For small-angle XRD analysis, the data were collected in reflection mode in the 2θ range from 0.7 to 6° with a step 0.5° (step time of 15s). For wide-angle XRD analysis, the data were collected in the 2θ range from 20 to 80° with a step of 0.5° (step time of 6s).

The nitrogen physisorption experiments were performed on a QUADRASORB SI gas sorption system (Quantachrome Instruments) in static measurement mode. Prior to the measurements, the samples were outgassed under high vacuum at 363K for 10h. The adsorption/desorption isotherms were obtained at 77K by allowing 4 min for equilibration between each successive point. The pore size distribution curves were calculated from the adsorption branches of the isotherms using Barrett-Joyner-Halenda (BJH) method. The BET surface area was determined using the multipoint algorithm. To evaluate the metal oxide phase assembling mode inside the pores of mesostructured silica support, the normalized BET and micropore surface area of catalyst were also calculated.[1] The mesopore size distribution was determined from the desorption branch of the isotherms using a nonlocal density functional theory (NL-DFT). The pore size diameter of the primary mesopores was determined at the maximum differential pore volume registered in the pore size distribution profiles. Transmission electron microscopy (TEM) was performed using a JEM-2010 at an acceleration voltage of 120 kV. FT-IR spectra were recorded on a Thermo Nicolet Nexus 470-FT-IR spectrometer using KBr pellets. The thermogravimetric analysis (TGA) was performed on a Perkin-Elmer Pyris Diamond TG instrument at a heating rate of 10℃/min under nitrogen atmosphere.

2. Experiment Procedures and Characterization Data

2.1 The Preparation of Ionic Liquid Monomer

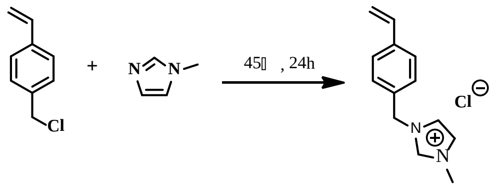

Ionic liquid, 1-(p-vinylbenzyl)-3-methylimidazolium chloride ([VBMI][Cl]), was synthesized according to a method reported by He *et al.*[2] Typically, a mixture of 4-(chloromethyl)styrene (1.53g, 10.0 mmol) and 1-methylimidazole (0.82g, 10.0 mmol) was stirred at 45 ℃ for 24 h under nitrogen atmosphere (Scheme 1). The reaction mixture was cooled down to room temperature, and the resultant precipitate was collected by filtration and washed with ethyl acetate (3×15 mL) and then dried at room temperature overnight under vacuum. ^{1}H NMR (mixture of $CDCl_3$ and CD_3OD, 400 MHz): 9.48 (1H, s, -N-CH-N-), 7,45-7.60 (6H, m, -N-CH-CH-N- and Ph), 6.73 (1H, dd, CH_2=CH-), 5.78 (1H, d, CH_2=CH-), 5.47 (2H, s, Ph-CH_2-N-), 5.32 (1H, d, CH_2=CH-), 3.99 (3H, s, -N-CH_3).

2.2 Preparation of SBA-PIL-Au catalyst

The preparation procedure of SBA-PIL-Au nanohybrids catalyst is schematically shown in Scheme 2.

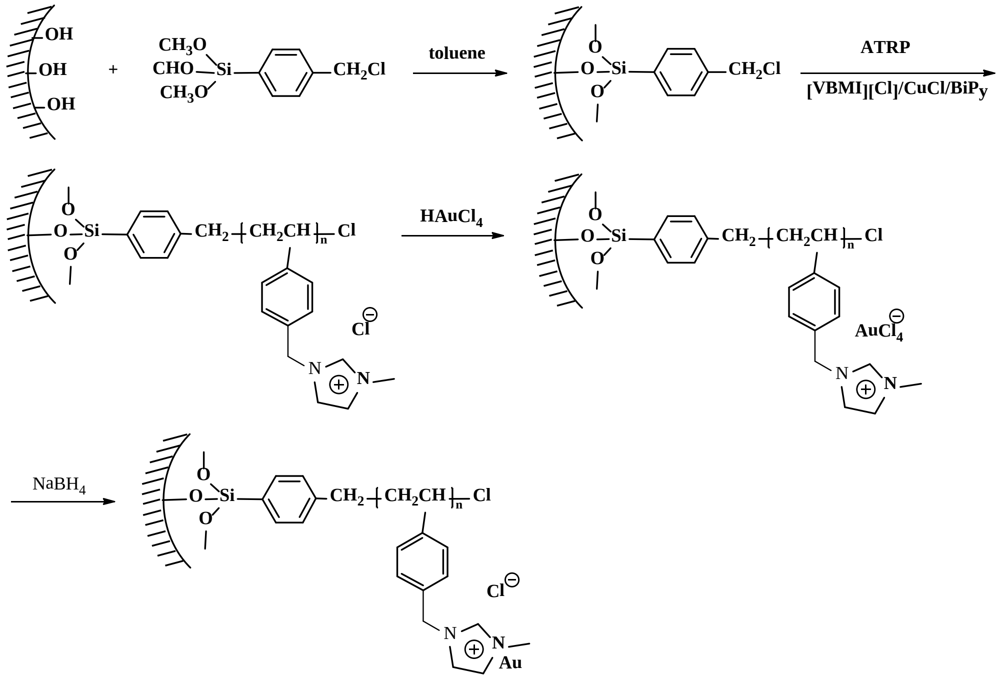

Scheme 2. Preparation of SBA-PIL-Au nanohybrid catalyst.

Immobilization of initiator on the SBA-15 surface (SBA-CTS)

The immobilization of SBA-15 with initiator was achieved according to a method reported by Li et al.[3] In order to generate a maximum number of silanol groups on the silica surface, the SBA-15 was refluxed in 17% HCl solution for 4 h. Two grams of acid treated SBA-15 were evacuated at 120 ℃ for 6 h and cooled down to room temperature. After that, a solution of 1.0 g of CTS in 40 mL of dry toluene containing 1.0 g pyridine was added to the treated SBA-15 under nitrogen atmosphere. The mixture was refluxed for 16 h under N_2 atmosphere. The solid was filtered and washed thoroughly with toluene to remove any unreacted CTS and other by-products. The CTS-immobilized SBA-15 was then washed with acetone and water. Finally, the solid was dried under vacuum at 100 ℃overnight, affording CTS modified SBA-15 support (SBA-CTS).

Preparation of Polymer-modified SBA-15 (SBA-PIL)

The surface-initiated polymerization of [VBMI][Cl] was carried out as follows: 1.0 g of SBA-CTS was sealed in a 100 mL Schlenk flask, and the flask was degassed by three vacuum purge/nitrogen fill cycles. 3.5 mg (0.025 mmol) of $CuCl_2$ and 7.8 mg (0.05 mmol) of BiPy were added to a round-bottom flask with a magnetic stirrer bar, and the round-bottom flask was also degassed by three vacuum purge/nitrogen fill cycles. A 40 mL degassed solution of [VBMI][Cl] monomer in DMF (degassed for 1 h) was then transferred to the above round-bottom flask. The mixture was well-stirred and heated with an oil bath to 50 ℃ until a transparent, light green solution formed. The obtained solution was then transferred into the Schlenk flask containing SBA-CTS to start the surface-initiated polymerization. After 12 hours' reaction at 50 ℃, the polymer modified substrate was removed from the Schlenk flask, washed with DMF and copious amount of water, the solid material was dried under vacuum at 100 ℃ overnight.

Preparation of SBA-PIL-Au catalyst

To prepare SBA-PIL-Au catalyst, 1.0 g of freshly prepared polymer-modified SBA-15 (SBA-PIL) was dispersed in 5.0 mL water. An aqueous $HAuCl_4$ solution (15.0 mL, 2.96 mM) was then added to the above suspension. The mixture was stirred for 0.5 h, and then filtered and washed several times with water. The recovered solid was re-dispersed in 10.0 mL H_2O, to which a 10.0 mL of freshly prepared $NaBH_4$ solution (0.2 M) was added under vigorous stirring to reduce Au^{3+}. After filtration and washing with copious amount of water, SBA-PIL-Au nanohybrid catalyst was obtained by overnight drying under vacuum at 80 ℃.

Oxidation of silanes

The oxidation of silanes was carried out in a two-phase system in a thermostatted two-neck round-bottom flask equipped with reflux condenser and magnetic stirrer. 3.0 mL water and a silane substrate (1.0 mmol) were added to the flask under vigorous stirring at 40 ℃. The reaction was started by the addition of a certain amount of catalyst. Reaction products were collected by a syringe in regular intervals and analyzed using a gas chromatograph (Agilent 7890A) equipped with an FID detector and a column of HP-5 (30m×0.0.32nm). The conversion and selectivity were obtained from the calibration curve. Ethylbenzene was used as internal standard.

Characterization of SBA- PIL-Au nanohybrids

The FT-IR spectra of SBA-15, SBA-CTS, and SBA-PIL are displayed in Figure S1. All materials exhibited a broad intense signal in the 1300-1000 cm^{-1} region corresponding to the characteristic Si-O-Si stretch adsorption. The FT-IR spectrum of SBA-CTS showed the vibration peaks at 2927 and 2854 cm^{-1}, which could be attributed to the CH_2 stretching vibrations of the aromatic ring, the band at 681 cm^{-1} could be assigned to the CH_2 groups on the CTS. For SBA-CTS, the bands at 1404, 1447, 1493 cm^{-1} were due to the vibrations of benzene ring. In addition to these peaks, the SBA-PIL also exhibited the new bands at 624, 3096 and 3150 cm^{-1}, which could be assigned to the vibrations of groups on poly(ionic liquid) brushes.

TGA was carried out for SBA-15, SBA-CTS, and SBA-PIL from 40 to 800 ℃ under nitrogen atmosphere (Figure S2). For all materials, the weight loss around 120 ℃was due to desorption of physic-absorbed water. In the range of 200-800 ℃, a weight loss of 4.5% for SBA-15 was ascribed to the desorption of water formed by the framework condensation. The weight loss of SBA-CTS and SBA-PIL between 120 and 700 ℃ was mainly due to the decomposition of the organic groups from the SBA-15. The SBA-CTS exhibited a weight loss of 15.1%, which was due to the loss of benzyl chloride functional group. In the range of 120-800 ℃, the weight loss of SBA-PIL was 29.5%.

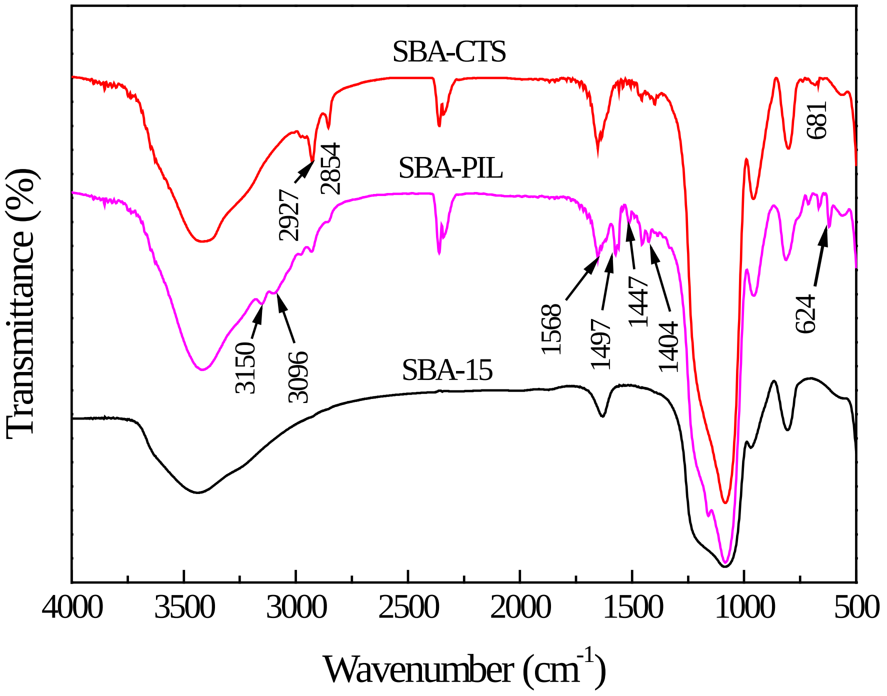

Figure S1. FT-IR spectra of SBA-15, SBA-CTS, and SBA-PIL materials.

Figure S3 displays the XRD patterns in the small-angle domain for the parent SBA-15, SBA-CTS, SBA-PIL, and SBA-PIL-Au nanoposites. All the patterns showed sharp diffraction peaks corresponding to the (100) planes as well as two less sharp peaks corresponding to the (110) and (200) planes at medium 2-theta angle range, suggesting that these materials had highly ordered 2-D hexagonal mesostructure. The XRD results showed that the mesostructure of SBA-15 did not change obviously during the postgrafting and the polymerization process. Compared with the pristine SBA-15, the SBA-CTS sample shows a very similar XRD pattern, while the intensity of (100) diffraction peak of SBA-PIL, and SBA-PIL-Au decreased. This may be caused partly by the decrease in the scattering intensity contrast between the channel pores and the walls of the mesoporous material, which suggests that the polymers were incorporated in the pore wall of SBA-15. Also, the polymer in the pore channels can deteriorate the mesoporous structure order. Moreover, it is obvious that the SBA-PIL sample shows a lower intensity of the (100) diffraction peak as compared with the SBA-PIL-Au, which is because the polymer shrinks considerably when adding AuCl^{4-},[4] suggesting that the majority of Au nanoparticles are highly dispersed and located within the mesopores of SBA-15.

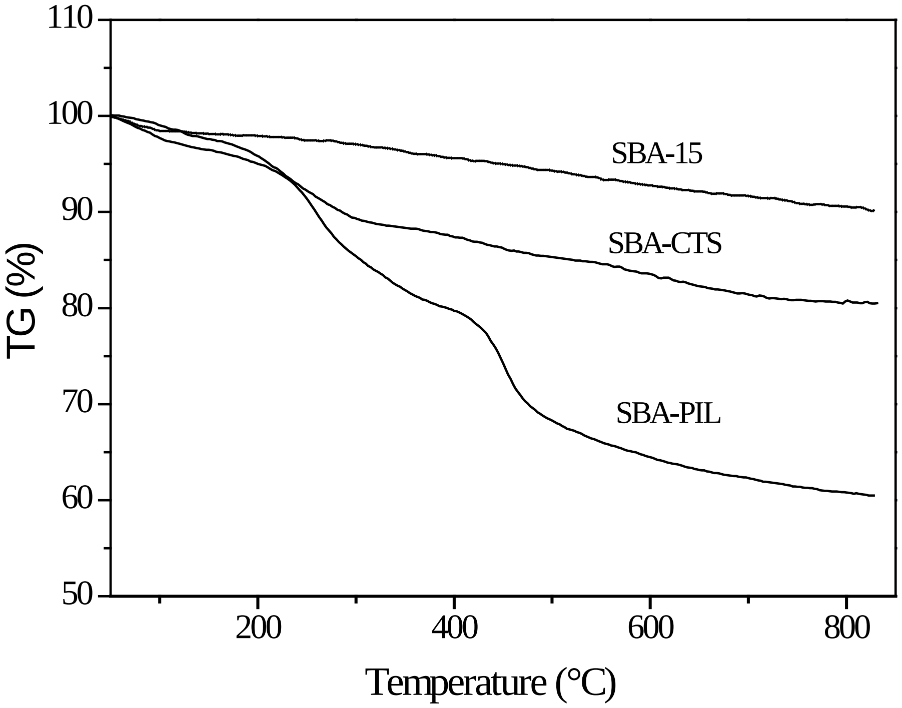

Figure S2. TGA curves of SBA-15, SBA-CTS, and SBA-PIL materials.

The textural properties of the materials were investigated by nitrogen adsorption/desorption measurements and the corresponding isotherms of SBA-15, SBA-CTS, SBA-PIL, and SBA-PIL-Au are shown in Figure S4.

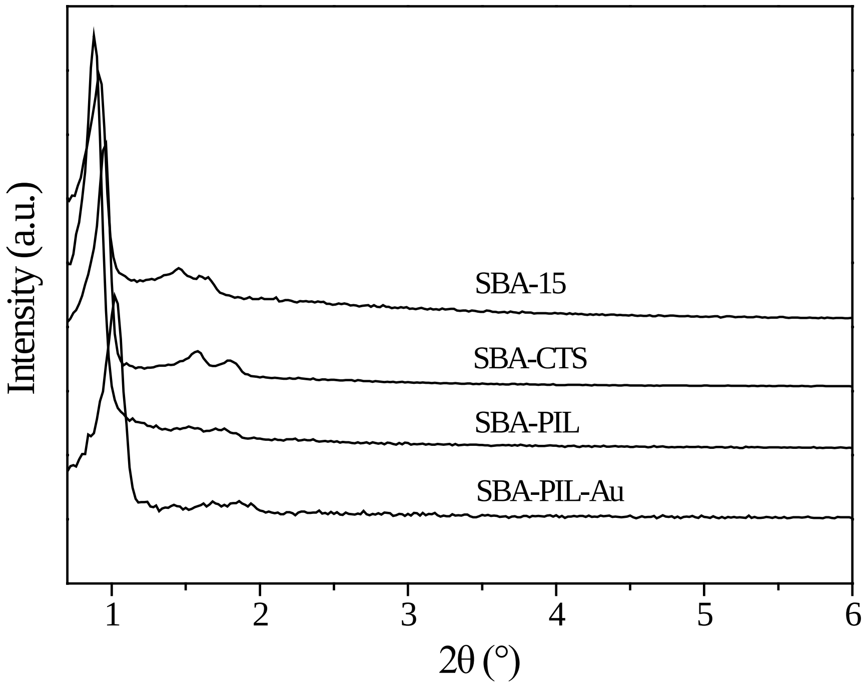

Figure S3. Low-angle XRD patterns between 0.7 and 5° for SBA-15, SBA-CTS, SBA-PIL, and SBA-PIL-Au materials.

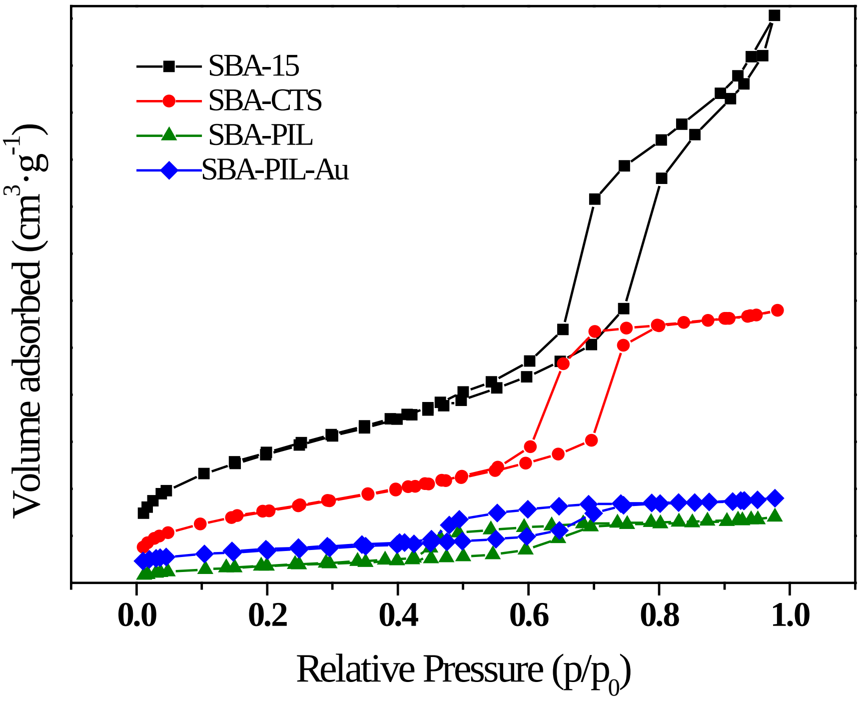

Figure S4. Nitrogen adsorption/desorption isotherms for SBA-15, SBA-CTS, SBA-PIL, and SBA-PIL-Au nanohybrids.

All samples showed the typical type IV isotherms with H1 hysteresis loops, which reveals that the highly ordered mesoporous SBA-15 solids have a narrow pore size distribution of the cylindrical channels, in good agreement with the results obtained by low-angle XRD. Similarly, it is noticed that the SBA-CTS sample displays an isotherm similar in shape with that of pristine SBA-15, which is characterized by steep adsorption/desorption branches and uniform H1 hysteresis loops at relative pressures (p/p0) of ~ 0.6-0.8, indicating that these materials essentially retain the initial texture of the pristine SBA-15. In contract to the pristine SBA-15, the SBA-PIL and SBA-PIL-Au show isotherms with less steep adsorption/desorption branches and capillary condensation steps shifted at relatively low pressure, which is due to the modification of poly(ionic liquid) and the subsequent formation of Au NPs. The obtained pore size distribution curves (Figure S5) are in close agreement with that of the adsoption/desorption isotherms. Thus, the materials display narrow pore size distributions in an order of SBA-15 > SBA-CTS > SBA-PIL-Au > SBA-PIL, in agreement with the result of lower-angle XRD, as already discussed above. On the basis of the adsorption/desorption isotherms, the textural properties of these materials were calculated by specific algorithms and summarized in Table S1. It can be observed that as compared with the pristine SBA-15, the BET of the modified SBA-15 decreased from 732 to 415, 119 and then increased to 152 $m^2 \cdot g^{-1}$, respectively. In parallel, the pore diameter and pore volume decreased from 9.5 nm and 1.25 m3·g-1 to 7.8 nm and 0.67 $m^3 \cdot g^{-1}$, 5.5 nm and 0.20 $m^3 \cdot g^{-1}$ and then increased to 7.5 nm and 0.25 $m^3 \cdot g^{-1}$, respectively. Similarly, the BET, pore diameter and pore volume for SBA-PIL-Au nanohybrids are higher than those of SBA-PIL precursor, as discussed in the XRD analysis.

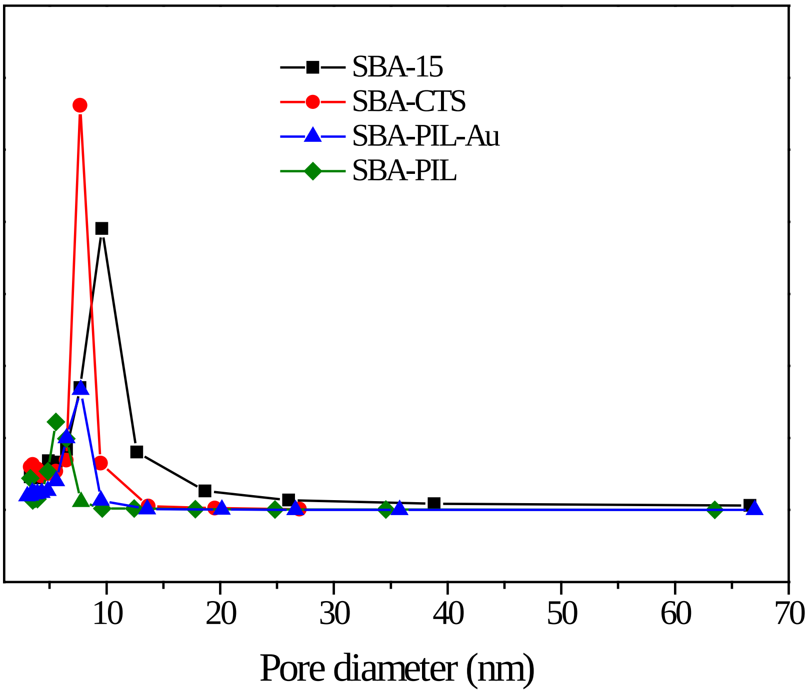

Figure S5. Pore size distribution for SBA-15, SBA-CTS, SBA-PIL, and SBA-PIL-Au nanohybrids.

Table S1: Physical properties of the pristine and modified SBA-15 materials.

Sample	BET surface area ($m^2.g^{-1}$)	Pore diameter (nm)	Pore vol.($m^3.g^{-1}$)
SBA-15	732	9.5	1.25

SBA-CTS	415	7.8	0.67
SBA-PIL	119	5.5	0.20
SBA-PIL-Au	152	7.5	0.25

XRD patterns recorded in the wide-angle domain for these materials are shown in Figure S6. Both the freshly prepared SBA-PIL-Au and the same sample reused for 4 times present a broad diffraction line at 38.2°, which can be indexed as gold (111) reflections.[5] The average size of the Au NPs after reused 4 times (Figure S6 b, 3.4 nm) calculated according to the (111) reflection peaks by Scherrer's equation, is found to be no remarkably increased compared to the freshly prepared Au catalyst (Figure S6a, 2.5 nm). This is an indication of good stability of SBA-PIL-Au after the reuse in oxidation reactions. The result indicates that the present of poly(ionic liquid) prevents the gold NPs from agglomeration effectively.

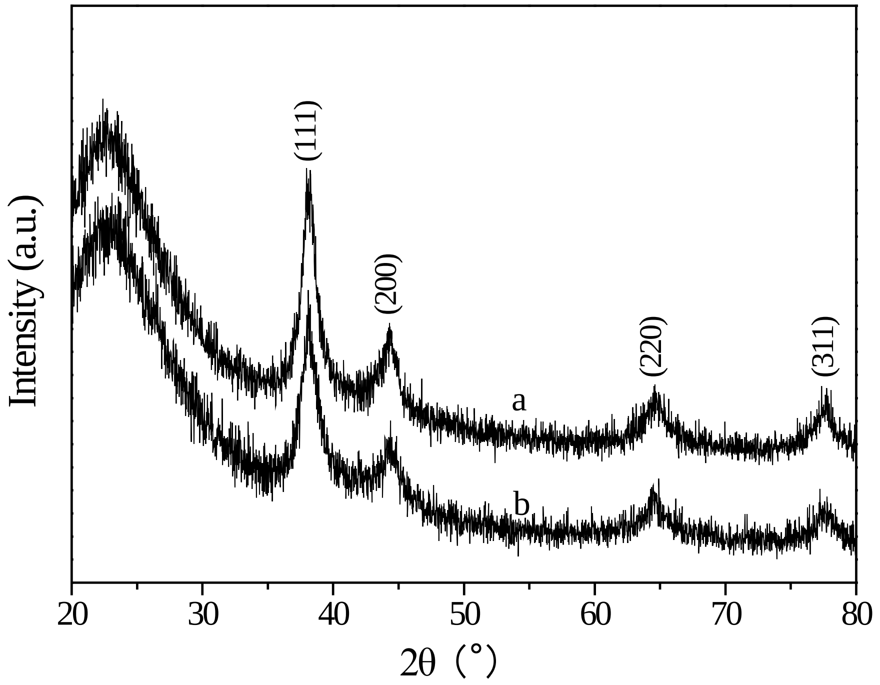

Figure S6. High-angle XRD patterns between 20 and 80° for (a) freshly prepared SBA-PIL-Au and (b) SBA-PIL-Au nanohybrids reused for 4 times.

Table S2: Comparing of SBA-PIL-Au with previous results with similar catalytic systems.

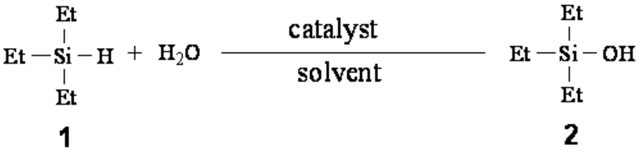

Catal.	Sub.(mmol)	Au/Sub. (mol%)	Sol.	Temp. (℃)	Time (min)	Conv. (%)	TON	TOF(h^{-1})
SBA-PIL-Au[a]	1.0	0.4	Acetone	40	60	4	25[b]	150[b]
SBA-PIL-Au[a]	1.0	0.4	EA	40	60	14	150[b]	900[b]
SBA-PIL-Au[a]	1.0	0.4	THF	40	60	25	200[b]	1200[b]
SBA-PIL-Au[a]	1.0	0.4	H_2O	40	60	>99	1500[b]	9000[b]
AuHAP[c]	1.0	0.83	H_2O	80	120	>99	120	40
NPs Au[d]	1.0	1.0	Acetone	RT	120	>94	10058	5029
AuCNT[e]	0.2	0.001	THF	RT	15	99	72000	12000
AuCNT[e]	0.2	0.005	THF	RT	60	99	18000	18000

[a] Reaction conditions: triethylsilane (1.0 mmol), water (0.1 mL), solvent (3.0 mL), air atmosphere, 40℃. [b] TOF was calculated by the conversion at initial 10 min and by assuming the surface gold atoms are active sites, and the surface gold atoms were evaluated by the dispersion of particles according to the equation: dispersion (%) = 1/d*100, where d refers to the average particles size measured with XRD. [c] Ref 6, [d] Ref 7, [e] Ref 8.

2.3 Reference

(1) a) K. Matyjaszewski, J. H. Xia, Chem. Rev. **2001**, *101*, 2921; b) S. Marc, P. Sebastian, M. Yu, K. Rhett, Adv. Mater, **2008**, *20*, 1928.

(2) X. Y. He, W. Yang, X. W. Pei, Macromolecules, **2008**, *41*, 4615.

(3) C. M. Li, J. Yang, P. Y. Wang, J. Liu, Q. H. Yang, Micropor. Mesopor. Mater, **2009**, *123*, 228.

(4) S. Marc, P. Sebastian, M. Yu, K. Rhett, M. Nobuyoshi, B. Matthias, Adv. Mater, **2008**, *20*, 1928.

(5) (a) A. Q. Wang, Y. P. Hsieh, Y. F. Chen, C. Y. Mou, J. Catal, **2006**, *237*, 197; (b) I. Robinson, L. D. Tung, S. Maenosono, C. Waltid, N. T. K. Thanh, Nanoscale, **2010**, *2*, 2624.

(6) T. Mitsudome, S. Arita, H. Mori, T. Mizugaki, K. Jitsukawa, K. Kaneda, Angew. Chem. Int. Ed., **2008**, *47*, 7938.

(7) N. Asao, Y. Ishikawa, N. Hatakeyama, Menggenbateer, Y. Yamamoto, M. W. Chen, W. Zhang, A. Inoue, Angew. Chem. Int. Ed., **2010**, *49*, 10093.

(8) J. John, E. Gravel, A. Hagge, H. Y. Li, T. Gacoin, E. Doris, Angew. Chem. Int. Ed., **2011**, *50*, 7533.